Published in final edited form as:
Curr Biol. 2012 August 7; 22(15): 1410–1416. doi:10.1016/j.cub.2012.05.035.

Tropomyosin Is Essential for Processive Movement of a Class V Myosin from Budding Yeast

Alex R. Hodges[1], **Elena B. Krementsova**[1], **Carol S. Bookwalter**[1], **Patricia M. Fagnant**[1], **Thomas E. Sladewski**[1], and **Kathleen M. Trybus**[1,*]

[1]Department of Molecular Physiology and Biophysics, University of Vermont, Burlington, VT 05405, USA

Summary

Myosin V is an actin-based motor protein involved in intracellular cargo transport [1]. Given this physiological role, it was widely assumed that all class V myosins are processive, able to take multiple steps along actin filaments without dissociating. This notion was challenged when several class V myosins were characterized as nonprocessive in vitro, including Myo2p, the essential class V myosin from *S. cerevisiae* [2–6]. Myo2p moves cargo including secretory vesicles and other organelles for several microns along actin cables in vivo. This demonstrated cargo transporter must therefore either operate in small ensembles or behave processively in the cellular context. Here we show that Myo2p moves processively in vitro as a single motor when it walks on an actin track that more closely resembles the actin cables found in vivo. The key to processivity is tropomyosin: Myo2p is not processive on bare actin but highly processive on actin-tropomyosin. The major yeast tropomyosin isoform, Tpm1p, supports the most robust processivity. Tropomyosin slows the rate of MgADP release, thus increasing the time the motor spends strongly attached to actin. This is the first example of tropomyosin switching a motor from nonprocessive to processive motion on actin.

Results and Discussion

Tropomyosin Is Essential for Processivity

We tested the hypothesis that Myo2p, which does not move processively on bare skeletal muscle actin in vitro, will move processively on a track that more closely resembles that found within the cell. In budding yeast, Myo2p moves on actin cables, which consist of multiple cross-linked actin filaments and several actin cross-linking and binding proteins, including fimbrin (Sac6p) and tropomyosin [7] (reviewed in [8]). To more closely mimic the track that Myo2p walks on in the cell, we first tested Myo2p function in vitro on single yeast actin filaments in the presence of tropomyosin (see Figure S1 available online). Yeast actin is only 87% identical to skeletal muscle actin and has half as many acidic residues (two versus four) near the N terminus, a region that plays an important role in the initial weak electrostatic interaction between actin and myosin. Tropomyosin is an α-helical coiled-coil that binds end-to-end along the actin filament [9]. Tpm1p is the most abundant tropomyosin isoform in yeast (~80% of the total) and is essential for actin cable formation [7, 10]. Here

*Correspondence: kathleen.trybus@uvm.edu.

Supplemental Information

Supplemental Information includes three figures, Supplemental Experimental Procedures, and two movies and can be found with this article online at doi:10.1016/j.cub.2012.05.035.

we used total internal reflection fluorescence (TIRF) microscopy to observe the interaction of single Myo2p motors with yeast actin filaments in the presence or absence of Tpm1p.

A truncated, constitutively active version of Myo2p lacking the globular tail (hereafter called Myo2p) was attached to streptavidin-coated quantum dots (Qdots) via a C-terminal biotin tag (Figure S1) [11]. A mixing ratio of 1 dimeric motor per 10 Qdots was used to ensure that moving Qdots were driven by a single motor (Figure S2). The Myo2p-Qdot mixture was added to rhodamine-labeled yeast actin filaments that were attached to a glass coverslip (Figure 1A).

In the absence of tropomyosin, no processive runs were observed, in agreement with previous results [2, 6]. Strikingly, when the experiment was repeated in the presence of Tpm1p, robust processivity was observed (Figure 1B; Movie S1). Qdot-labeled Myo2p moved along actin-Tpm1p filaments for micron scale distances. The run length histogram (n = 255 processive runs) was fit with an exponential curve ($y = Ae^{-x/\lambda}$) to determine the characteristic run length λ λ = 0.89 μm (Figure 1C).

The average speed during processive motion was 5.4 ± 1.1 μm/s (mean ± SD) (Table 1), approximately 10-fold faster than vertebrate myosin Va (myoVa), which moved at ~0.60 μm/s in control experiments. The entire ATPase cycle, especially the rate-limiting step, must be correspondingly faster for Myo2p than myoVa.

During processive motion, individual steps of the motor were clearly resolved when the speed of Myo2p was slowed by reducing the ATP concentration to 2 μM (Figure 1D). A total of 169 steps were observed, including four backward steps. The step size distribution was roughly Gaussian, centered at 34.1 ± 1.3 nm (mean ± SE), consistent with a hand-over-hand mechanism in which each head alternately takes a 72 nm step (Figure 1E) [12–14]. As for other class V myosins, the repeat of the actin filament dictates the step size. The width of the distribution was fairly large (SD = 14 nm), which is either an inherent property of Myo2p or due to experimental uncertainty in the position measurement. The latter is possible given that the motor was labeled with a Qdot at the end of the flexible coiled-coil domain, which results in a noisier signal than if the Qdot is bound to the N-terminal motor domain and closer to actin.

Actin Bundling Increases Myo2p Run Length but Reduces Speed

To more closely mimic the actin cables that Myo2p walks on in the cell, we observed Myo2p behavior on yeast actin-fascin bundles. Fascin is an actin cross-linking protein that results in bundles of parallel actin filaments separated by ~9 nm [15]. At high MgATP concentration (2 mM), Myo2p is not processive on actin-fascin bundles in the absence of tropomyosin. On yeast actin-Tpm1p-fascin bundles, processive movement was observed with an average speed of 2.9 ± 0.9 μm/s and a run length of 1.11 ± 0.14 μm (Figure S3). Relative to single actin-Tpm1p filaments, actin bundling resulted in a ~35% reduction in speed and a ~40% increase in run length. The observed speed of 2.9 μm/s on actin bundles is in good agreement with the 2–3 μm/s speeds observed for Myo2p driven secretory vesicles in vivo [6, 16]. The multiple actin filaments in a bundle provide an increased number of target actin binding sites, which potentially allows Myo2p to step onto adjacent filaments as observed for myosin X, a motor adapted for processive motility on bundled actin [17]. These additional binding sites would allow Myo2p to take shorter steps and consequently move slower [17–19]. Stepping onto adjacent filaments would also affect the intramolecular strain between the two heads because of the addition of off-axis components, thus potentially affecting gating.

Tropomyosin Isoform Matters

Two other tropomyosin isoforms were tested, one from yeast and one from a vertebrate. Budding yeast contains a second, less abundant tropomyosin isoform called Tpm2p. Both yeast tropomyosins are notable in that they are short, spanning only four (Tpm2p) or five (Tpm1p) actin monomers, in contrast to tropomyosins from higher eukaryotes, which span six or seven actin monomers.

The speed of movement on yeast actin-Tpm2p (5.2 ± 1.2 μm/s, mean ± SD) was not significantly different than that with Tpm1p ($p = 0.25$), but the run length was reduced by ~25%, and the frequency of processive runs was reduced 2-fold (Figure 1C; Table 1; Movie S1). Chicken gizzard smooth muscle tropomyosin also supported processive runs, but Myo2p function was impaired relative to either yeast tropomyosin. Average speed was 4.6 ± 1.4 μm/s (mean ± SD), which is significantly lower than for Tpm1p or Tpm2p ($p < 0.01$ for both). Run length was also reduced by 40% to 0.53 μm, and the frequency of processive runs was 10-fold lower than with Tpm1p (Figure 1C; Table 1).

Although all three tropomyosins tested supported processive movement of Myo2p, it is not surprising that Tpm1p, the isoform found on actin cables in vivo, gave the highest run frequency and the longest run lengths for Myo2p. Next most effective was yeast Tpm2p, whose in vivo role is less clear, although there is evidence that it is associated with type II myosin [20]. Smooth muscle tropomyosin, which differs the most from the yeast isoforms, was the least effective. These differences imply a direct interaction of Myo2p with tropomyosin, rather than a general allosteric change in the actomyosin interface mediated by tropomyosin. Tpm1p, which localizes to and stabilizes actin cables in yeast, is thus optimized for its cellular role of supporting Myo2p function as a cargo transporter.

Actin Isoform Does Not Matter

In the absence of tropomyosin, neither skeletal muscle actin nor yeast actin supported processive runs. Decorating skeletal actin with yeast Tpm1p, however, restored the ability of Myo2p to move processively with an average speed of 5.4 ± 1.4 μm/s (mean ± SD) and run length of 0.77 μm, nearly identical to the results with yeast actin-Tpm1p (Table 1; Figure S3). In agreement with our results, a recent study showed that the speed at which Myo2p moved bare actin filaments in an ensemble gliding filament motility assay was the same for yeast and skeletal muscle actin [21].

Electron microscopy and image reconstruction showed that all tropomyosins characterized so far occupy either the blocked or closed states on actin, in the absence of myosin and troponin, a striated muscle regulatory protein. In the blocked state, tropomyosin sterically prevents myosin from binding to actin, whereas in the closed state, myosin can bind weakly. Further myosin binding cooperatively shifts tropomyosin to the open state, which fully exposes the myosin binding site. Actin isoform has been shown to affect tropomyosin position. Skeletal muscle tropomyosin is in the closed state on skeletal muscle actin, but in the blocked state on yeast actin [22]. Yeast Tpm1p is also in the closed state on skeletal muscle actin, but its position on yeast actin was not determined [22]. We did not observe any effects of actin isoform on Myo2p behavior at the single molecule level.

Effect of Tpm1p on Myo2p Kinetics

For a two-headed motor to be processive, it must have a duty ratio of greater than 50%. That is, each head must spend more than half of its ATPase cycle strongly bound to its track, thus preventing simultaneous detachment of both heads [23]. This feature, known as a high duty ratio, is sufficient to obtain processive motion. Further enhancement of run length results from communication between the heads, which puts their kinetic cycles out of phase as a

result of intramolecular strain between the two actin-bound heads (reviewed in [24]). This "gating" between heads enhances processivity by preventing premature dissociation of the leading head. The prototypical processive myosin motor, vertebrate myoVa [25], achieves a high duty ratio by having ADP dissociation as the rate-limiting step in the ATPase cycle, given that myoVa.ADP has a high affinity for actin [26]. Once the rear head releases ADP and binds ATP, it detaches from actin and swings forward, relieving intramolecular strain. The new leading head undergoes a diffusive search for its next actin binding site, ~72 nm farther along the filament. This reattachment step, which involves weak binding to actin followed by phosphate release, must be fast relative to the ADP release rate to ensure long run lengths [11, 27].

Myo2p was reported to have only ~20% duty ratio in the absence of tropomyosin [2], which is incompatible with processivity. Therefore, we hypothesized that tropomyosin increases the duty ratio of Myo2p by changing its kinetics: either slowing down ADP release, speeding up phosphate release, or both. The strain-based gating seen with myoVa is likely to be retained by Myo2p given the similar molecular architecture of the two motors.

To determine the effect of tropomyosin on Myo2p kinetics, we used a single-headed construct truncated after the second IQ domain, Myo2p-2IQ (Figure S1). Skeletal actin was used for the kinetic assays because our single molecule results showed no difference between yeast and skeletal actin, and it was difficult to express sufficient quantities of yeast actin for these studies. The steady-state actin-activated ATPase activity of Myo2p was determined in the presence or absence of Tpm1p with skeletal actin (Figure 2A). Fits to Michaelis-Menten kinetics showed a slight reduction of the maximal ATPase rate with Tpm1p (V_{max} = 171 ± 4 s^{-1}, actin only; V_{max} = 151 ± 4 s^{-1}, actin-Tpm1p) and similar values for the actin concentration at half-maximal velocity (K_M = 39 ± 2 μM, actin only; K_M = 34 ± 2 μM, actin-Tpm1p).

Transient kinetics were next used to determine whether tropomyosin affects the rate of ATP-induced dissociation of the motor from actin or the rate of ADP release. Acto-Myo2p-2IQ (±Tpm1p) was mixed with varying MgATP concentrations in a stopped-flow spectrophotometer. The decrease in light scattering was used to follow the MgATP-induced dissociation of Myo2p-2IQ from actin, and single exponentials were fit to the resulting transients. Tpm1p caused a 47% reduction in the maximal ATP dissociation rate from 467 ± 39 s^{-1} to 246 ± 22 s^{-1} (Figure 2B). To measure the rate of ADP dissociation, acto-Myo2p-2IQ with varying MgADP concentrations (±Tpm1p) was mixed with 6mMMgATP. Light scattering was used to follow the MgATP-induced dissociation of Myo2p-2IQ from actin, which can only occur after MgADP is released from the active site. Myo2p did not quench actin pyrene fluorescence in the strongly bound state, nor did mant-ADP show a large fluorescence change upon binding, precluding the use of these methods to measure ADP release. The apparent ADP dissociation rate was measured at 3 MgADP concentrations (Figure 2C). The presence of Tpm1p reduced the observed rate from 238 s^{-1} to 144 s^{-1} at 600 μM ADP. This apparent ADP dissociation rate includes contributions from ATP binding as well as ADP release, because ATP-induced dissociation of the actomotor complex is relatively slow for Myo2p-2IQ. The value represents the rate at which Myo2p-2IQ transitions from strongly bound (Acto-Myo2p-2IQ.ADP) to weakly bound (actin + Myo2p-2IQ.ATP) states.

Taken together, the steady-state and transient kinetic data suggest that the major effect of tropomyosin is to increase the duty ratio of Myo2p. In the presence of Tpm1p, the steady-state ATPase rate is essentially the same as the ADP release rate (151 s^{-1} versus 144 s^{-1}). ADP dissociation and ATP-induced dissociation of the actomotor complex are the rate-limiting steps in the ATPase cycle, and Myo2p spends the majority of the cycle in a strongly

bound state. In the absence of Tpm1p, the steady-state ATPase rate is slower than the ADP dissociation rate (171 s^{-1} versus 238 s^{-1}), and thus Myo2p spends a substantial portion of each ATPase cycle in weakly bound states.

Tpm1p reduced the steady state ATPase rate to a lesser extent than the apparent ADP dissociation rate, implying that another rate in the ATPase cycle (e.g., phosphate release) may be increased to compensate and keep the overall cycle time similar. The discrepancy may also arise because tropomyosin is in different positions on actin for the transient kinetics assays versus the steady-state ATPase assays. The steady-state ATPase measurements are performed in MgATP with a low ratio of motor to actin, and thus most Tpm1p will be in the blocked or closed states. In contrast, the transient kinetic measurements start with actin filaments saturated with strongly bound motors, which would push Tpm1p into the open position. The single molecule assays suggest, however, that the starting tropomyosin position may not be so critical. Typically, actin filaments were attached to the coverslip with NEM myosin (an ATP-insensitive skeletal muscle myosin), which would also push Tpm1p toward the open state. Experiments in which yeast actin-Tpm1p filaments were attached nonspecifically to polylysine-coated coverslips, with Tpm1p presumably in the closed or blocked position, gave nearly identical results (Figure S3). It has been proposed that the energy barriers between the different tropomyosin configurations are low in the absence of troponin [22]. Thus it is probably not energetically costly for Myo2p to displace tropomyosin to the open position as it binds to and steps along the actin filament.

Tropomyosin Increases Run Lengths at Low ATP

The kinetic data suggest that the primary effect of tropomyosin is to increase the duty ratio of Myo2p. In support of this hypothesis, artificially increasing the duty ratio by reducing the ATP concentration allowed Myo2p to move processively on both bare actin filaments and actin-Tpm1p filaments (Figure 3; Movie S2). ATP binding occurs at ~1×10^6 $M^{-1}sec^{-1}$, so that at 10 μM ATP this becomes the rate-limiting step in the ATPase cycle. The overall cycle time is increased and Myo2p spends the majority of the ATPase cycle strongly bound to actin in an apo-state, waiting for ATP to bind.

At 10 μM ATP, the speed is 0.19 ± 0.05 μm/s (yeast actin only) or 0.18 ± 0.04 μm/s (yeast actin-Tpm1p), a ~30-fold reduction compared to the speed at 2 mM ATP. Surprisingly, actin-Tpm1p supports much longer run lengths than bare actin (5.1 μm versus 1.5 μm, Figure 3B). Because ATP binding dominates the cycle, the predicted duty ratio of Myo2p is >95% for both cases, and we expected essentially identical behavior unless tropomyosin also does something more. A possible explanation for the run length enhancement is that tropomyosin improves gating between the two Myo2p heads by slowing ADP release from the lead head.

Additional Factors that Promote Processivity

Both isoforms of myosin V from budding yeast, Myo4p and Myo2p, were characterized as nonprocessive in vitro, because they lacked a critical component that is present in vivo. For Myo2p, we show here that the difference is tropomyosin. For Myo4p, the “processivity factor” is the oligomeric cargobinding adaptor protein She2p, which is required to dimerize the single-headed motor Myo4p [28]. Although tropomyosin is not essential for Myo4p processivity, it did increase the run frequency [28]. Other class V myosins, including human myosin Vc and *Drosophila* myosin V, are also nonprocessive in vitro on bare actin filaments [3–5]. We speculate that they may be processive with the proper tropomyosin or some other missing component. In contrast, the highly processive vertebrate myoVa seems to be largely unaffected by tropomyosin, based on a study that showed that chick brain myoVa motility was unaffected by skeletal muscle tropomyosin [29].

Previously we showed that the kinesin family protein Smy1p acts as a tether to enhance Myo2p function [6]. When Smy1p and Myo2p are attached to the same cargo, Smy1p interacts electrostatically with actin and allows a single Myo2p motor to move continuously along a bare actin filament (without tropomyosin) for several microns. However, we were unable to detect discrete steps in the position versus time data and thus concluded that Smy1p did not promote true processive hand-over-hand stepping [6]. Myo2p most likely dissociates after each step, whereas Smy1p anchors the cargo to the actin track, resulting in a biased one dimensional diffusion along the actin. In support of this argument, the average speed of the Smy1p-Myo2p complex along bare actin filaments is approximately 4-fold slower than the speed of Myo2p along actin-Tpm1p filaments (1.4 μm/s versus 5.4 μm/s). Although Smy1p probably enhances Myo2p processivity in vivo, it is not essential like tropomyosin is.

Conclusions

Although the role of tropomyosin-troponin is well understood in striated muscle, less is known about how tropomyosin affects myosin function in nonmuscle cells, even though cytoplasmic actin has tropomyosin bound (reviewed in [30]). Tropomyosin is usually thought of as inhibiting actomyosin interactions, as it does in skeletal muscle and for type I myosins [31, 32]. However, various nonmuscle and smooth muscle tropomyosin isoforms have also been shown to increase myosin ATPase rates and motility [30, 32–36]. Here we provide the first example of tropomyosin enhancing a class V myosin function to the extent that a nonprocessive motor can now walk processively as a single motor at millimolar ATP concentration. More than for any other class V myosin, the role of Myo2p as a cargo transporter in vivo is clear, and thus its processivity within the cell makes biological sense. Kinetically, the primary effect of tropomyosin is to increase the duty ratio of Myo2p by slowing the ADP dissociation and ATP binding rates. This ensures that each head spends a greater fraction of its ATPase cycle strongly attached to actin, thus enabling processive motion (summarized in Figure 3C). A secondary effect may be enhancement of the gating between heads, which further increases run length.

An optimum pairing of motor and track could help target the appropriate myosin to the proper population of actin filaments in the cell, thus providing the strong potential for both spatial and temporal regulation of myosin function [9, 30, 32, 37]. Our data with proteins from a simple organism like budding yeast support the idea that motor function is sensitive to the tropomyosin isoform. The potential for specific regulation of motor activity is even greater in higher eukaryotes like humans, where there are over 40 isoforms of tropomyosin, as well as at least 10 classes of myosin motors, each with multiple isoforms.

Experimental Procedures

TIRF Microscopy and Data Analysis

For experiments performed at 2 mM ATP, Myo2pΔGT (0.2 μM) was mixed with a 2-fold molar excess of actin and 2 mM MgATP, and centrifuged for 20 min at 400,000 *g* to remove any myosin that was unable to dissociate from actin in the presence of ATP. The supernatant was then mixed with a 10-fold excess of 655 nm streptavidin-coated quantum dots (Qdots, Invitrogen) to ensure that Qdots were transported by a single Myo2p. Flow cells made from glass coverslips were prepared by introducing the following solutions into the flow cell: 0.1 mg/ml *N*-ethylmaleimide-modified skeletal muscle myosin (5 min incubation), 5X rinse of 1 mg/ml BSA (2 min), rhodamine-phalloidin-labeled yeast or chicken skeletal muscle actin filaments (plus or minus 1 μM tropomyosin) (2–5 min), 5X rinse with motility buffer, and, finally, 0.2 nM Myo2p in motility buffer with 2 mM MgATP. Motility buffer consists of 50 mM KCl, 25 mM imidazole, pH 7.4, 4 mM $MgCl_2$, 1 mM EGTA, 50 mM dithiothreitol

(DTT), 1 mg/ml BSA, 0.2 mg/ml yeast calmodulin, 0.2 mg/ml Mlc1p, an ATP regenerating system (0.5 mM phosphoenolpyruvate and 100 U/ml pyruvate kinase), and an oxygen-scavenging system (3 mg/ml glucose, 0.1 mg/ml glucose oxidase, and 0.18 mg/ml catalase). For experiments with tropomyosin, 1 μMtropomyosin was included in the motility buffer to prevent dissociation from actin. Experiments were performed at 22°C.

Through-the-objective TIRF fluorescence microscopy was performed at room temperature (22°C) using an inverted microscope (Eclipse Ti-U; Nikon) equipped with a 100× Plan Apo objective lens (1.49 NA) and auxiliary 1.5X magnification. The Qdots were excited with a 473 nm laser line. Images were obtained using an XR/Turbo-Z camera (Stanford Photonics) running Piper Control software (v2.3.39). The pixel resolution was 95.0 nm, and data were collected at 30–40 frames per s. Qdot movement along rhodamine-labeled actin filaments was tracked by hand using ImageJ. For each event, we required Qdot-labeled Myo2p to move continuously for at least 3 frames to qualify as a run. Runs artificially terminated by running off the end of an actin filament were not included in the run length analysis. To test whether Myo2p speed was affected by tropomyosin isoform, a Student's t test (two-tailed, two-sample unequal variance) was performed using Microsoft Excel.

For experiments performed at 10 μM ATP, the procedure was similar, except the Myo2p concentration was reduced to 10 or 20 pM and data were collected at 1 frame per s. Flow cells were sealed with grease to prevent evaporation. Only actin filaments at least 10 μm long were included in the analysis.

To determine Myo2p step size on yeast actin-Tpm1p filaments, the procedure was again similar, except the ATP concentration was 2 μM, the Myo2p concentration was 4 pM, and data were collected at 60 frames per s. Qdot position versus time was tracked using SpotTracker, an automated motion-tracking plugin for ImageJ [38]. Step sizes were calculated in MATLAB using the Kerssemakers step-finding algorithm [39].

Kinetic Assays

Steady-state actin-activated ATPase assays were performed at 25°C in 10 mM imidazole, pH 7.4, 50 mM KCl, 1 mM $MgCl_2$, 1mM EGTA, and 1 mM dithiothreitol. Reactions contained 8.5−12.7 nM Myo2p-2IQ and 0.1 mg/mL Mlc1p and yeast calmodulin (Cmd1p). Chicken skeletal F-actin was preincubated with Tpm1p at a 2:1 or 4:1 molar ratio, along with an additional 1 μMexcess Tpm1p, 60 min prior to dilution. Experiments using 2:1 or 4:1 actin-Tpm1p ratios gave identical results. Reactions were initiated by the addition of 2 mM MgATP. The buffers also contained an ATP regenerating system (0.5 mM phosphoenolpyruvate, 100 units/ml pyruvate kinase), 0.2 mM NADH, and 20 units/ml lactate dehydrogenase. The rate of the reaction was measured from the decrease in absorbance at 340 nm. Data were fit to the Michaelis-Menten equation to obtain V_{max} and K_M.

The stop-flow experiments were carried out on a Kintek SF-2002 stop-flow apparatus (Kintek, Austin, TX). Light scattering was measured with an exciting light of 294±10 nm and emission monitored with a 294 nm cutoff filter. The rate of ATP-induced dissociation of the actomotor complex was measured by mixing a solution containing 1 μM skeletal actin (±0.25 μM Tpm1p) and 0.7 μM Myo2p-2IQ, with a solution containing varying MgATP concentrations. The rate of ADP release was measured by mixing a solution containing 1 μM skeletal actin (±0.25 μM Tpm1p), 0.7 μM Myo2p-2IQ, and 200–600 μM MgADP with a solution of 6 mM MgATP. The light scattering traces were fit to single exponentials using software provided by Kintek. Buffer conditions were 10 mM imidazole, pH 7.4, 50 mM KCl, 1 mM $MgCl_2$, 1 mM EGTA, and 1 mM DTT at 25°C.

Constructs, Protein Expression, and Purification

Details on constructs, protein expression, and purification can be found in Supplemental Information.

Supplementary Material

Refer to Web version on PubMed Central for supplementary material.

Acknowledgments

The authors thank Matthew Lord for insightful discussions, Guy Kennedy for technical assistance, David Warshaw for use of the TIRF microscope, and Mushtaba Yuribdalla for contributing to the data analysis. This work was supported by funds from the National Institutes of Health (GM078097 to K.M.T.).

References

1. Trybus KM. Myosin V from head to tail. Cell Mol Life Sci. 2008; 65:1378–1389. [PubMed: 18239852]
2. Reck-Peterson SL, Tyska MJ, Novick PJ, Mooseker MS. The yeast class V myosins, Myo2p and Myo4p, are nonprocessive actin-based motors. J Cell Biol. 2001; 153:1121–1126. [PubMed: 11381095]
3. Tóth J, Kovács M, Wang F, Nyitray L, Sellers JR. Myosin V from Drosophila reveals diversity of motor mechanisms within the myosin V family. J Biol Chem. 2005; 280:30594–30603. [PubMed: 15980429]
4. Watanabe S, Watanabe TM, Sato O, Awata J, Homma K, Umeki N, Higuchi H, Ikebe R, Ikebe M. Human myosin Vc is a low duty ratio nonprocessive motor. J Biol Chem. 2008; 283:10581– 10592. [PubMed: 18079121]
5. Takagi Y, Yang Y, Fujiwara I, Jacobs D, Cheney RE, Sellers JR, Kovács M. Human myosin Vc is a low duty ratio, nonprocessive molecular motor. J Biol Chem. 2008; 283:8527–8537. [PubMed: 18201966]
6. Hodges AR, Bookwalter CS, Krementsova EB, Trybus KM. A nonprocessive class V myosin drives cargo processively when a kinesin- related protein is a passenger. Curr Biol. 2009; 19:2121– 2125. [PubMed: 20005107]
7. Pruyne DW, Schott DH, Bretscher A. Tropomyosin-containing actin cables direct the Myo2p-dependent polarized delivery of secretory vesicles in budding yeast. J Cell Biol. 1998; 143:1931–1945. [PubMed: 9864365]
8. Pruyne D, Legesse-Miller A, Gao L, Dong Y, Bretscher A. Mechanisms of polarized growth and organelle segregation in yeast. Annu Rev Cell Dev Biol. 2004; 20:559–591. [PubMed: 15473852]
9. Gunning PW, Schevzov G, Kee AJ, Hardeman EC. Tropomyosin isoforms: divining rods for actin cytoskeleton function. Trends Cell Biol. 2005; 15:333–341. [PubMed: 15953552]
10. Drees B, Brown C, Barrell BG, Bretscher A. Tropomyosin is essential in yeast, yet the TPM1 and TPM2 products perform distinct functions. J Cell Biol. 1995; 128:383–392. [PubMed: 7844152]
11. Hodges AR, Krementsova EB, Trybus KM. Engineering the processive run length of Myosin V. J Biol Chem. 2007; 282:27192–27197. [PubMed: 17640878]
12. Yildiz A, Forkey JN, McKinney SA, Ha T, Goldman YE, Selvin PR. Myosin V walks hand-over-hand: single fluorophore imaging with 1.5-nm localization. Science. 2003; 300:2061–2065. [PubMed: 12791999]
13. Warshaw DM, Kennedy GG, Work SS, Krementsova EB, Beck S, Trybus KM. Differential labeling of myosin V heads with quantum dots allows direct visualization of hand-over-hand processivity. Biophys J. 2005; 88:L30–L32. [PubMed: 15764654]
14. Forkey JN, Quinlan ME, Shaw MA, Corrie JE, Goldman YE. Three-dimensional structural dynamics of myosin V by single-molecule fluorescence polarization. Nature. 2003; 422:399–404. [PubMed: 12660775]

15. Ishikawa R, Sakamoto T, Ando T, Higashi-Fujime S, Kohama K. Polarized actin bundles formed by human fascin-1: their sliding and disassembly on myosin II and myosin V in vitro. J Neurochem. 2003; 87:676–685. [PubMed: 14535950]
16. Schott DH, Collins RN, Bretscher A. Secretory vesicle transport velocity in living cells depends on the myosin-V lever arm length. J Cell Biol. 2002; 156:35–39. [PubMed: 11781333]
17. Ricca BL, Rock RS. The stepping pattern of myosin X is adapted for processive motility on bundled actin. Biophys J. 2010; 99:1818–1826. [PubMed: 20858426]
18. Nagy S, Ricca BL, Norstrom MF, Courson DS, Brawley CM, Smithback PA, Rock RS. A myosin motor that selects bundled actin for motility. Proc Natl Acad Sci USA. 2008; 105:9616– 9620. [PubMed: 18599451]
19. Sun Y, Sato O, Ruhnow F, Arsenault ME, Ikebe M, Goldman YE. Single-molecule stepping and structural dynamics of myosin X. Nat Struct Mol Biol. 2010; 17:485–491. [PubMed: 20364131]
20. Huckaba TM, Lipkin T, Pon LA. Roles of type II myosin and a tropomyosin isoform in retrograde actin flow in budding yeast. J Cell Biol. 2006; 175:957–969. [PubMed: 17178912]
21. Stark BC, Wen KK, Allingham JS, Rubenstein PA, Lord M. Functional adaptation between yeast actin and its cognate myosin motors. J Biol Chem. 2011; 286:30384–30392. [PubMed: 21757693]
22. Lehman W, Hatch V, Korman V, Rosol M, Thomas L, Maytum R, Geeves MA, Van Eyk JE, Tobacman LS, Craig R. Tropomyosin and actin isoforms modulate the localization of tropomyosin strands on actin filaments. J Mol Biol. 2000; 302:593–606. [PubMed: 10986121]
23. Veigel C, Wang F, Bartoo ML, Sellers JR, Molloy JE. The gated gait of the processive molecular motor, myosin V. Nat Cell Biol. 2002; 4:59–65. [PubMed: 11740494]
24. Sellers JR, Veigel C. Walking with myosin V. Curr Opin Cell Biol. 2006; 18:68–73. [PubMed: 16378722]
25. Mehta AD, Rock RS, Rief M, Spudich JA, Mooseker MS, Cheney RE. Myosin-V is a processive actin-based motor. Nature. 1999; 400:590–593. [PubMed: 10448864]
26. De La Cruz EM, Wells AL, Rosenfeld SS, Ostap EM, Sweeney HL. The kinetic mechanism of myosin V. Proc Natl Acad Sci USA. 1999; 96:13726–13731. [PubMed: 10570140]
27. Dunn AR, Spudich JA. Dynamics of the unbound head during myosin V processive translocation. Nat Struct Mol Biol. 2007; 14:246–248. [PubMed: 17293871]
28. Krementsova EB, Hodges AR, Bookwalter CS, Sladewski TE, Travaglia M, Sweeney HL, Trybus KM. Two single-headed myosin V motors bound to a tetrameric adapter protein form a processive complex. J Cell Biol. 2011; 195:631–641. [PubMed: 22084309]
29. Wolenski JS, Cheney RE, Mooseker MS, Forscher P. In vitro motility of immunoadsorbed brain myosin-V using a Limulus acrosomal process and optical tweezer-based assay. J Cell Sci. 1995; 108:1489–1496. [PubMed: 7615669]
30. Ostap EM. Tropomyosins as discriminators of myosin function. Adv Exp Med Biol. 2008; 644:273–282. [PubMed: 19209828]
31. Tang N, Ostap EM. Motor domain-dependent localization of myo1b (myr-1). Curr Biol. 2001; 11:1131–1135. [PubMed: 11509238]
32. Clayton JE, Sammons MR, Stark BC, Hodges AR, Lord M. Differential regulation of unconventional fission yeast myosins via the actin track. Curr Biol. 2010; 20:1423–1431. [PubMed: 20705471]
33. Strand J, Nili M, Homsher E, Tobacman LS. Modulation of myosin function by isoform-specific properties of Saccharomyces cerevisiae and muscle tropomyosins. J Biol Chem. 2001; 276:34832–34839. [PubMed: 11457840]
34. Chacko S. Effects of phosphorylation, calcium ion, and tropomyosin on actin-activated adenosine 5′-triphosphatase activity of mammalian smooth muscle myosin. Biochemistry. 1981; 20:702–707. [PubMed: 6452159]
35. Sellers JR, Pato MD, Adelstein RS. Reversible phosphorylation of smooth muscle myosin, heavy meromyosin, and platelet myosin. J Biol Chem. 1981; 256:13137–13142. [PubMed: 6118372]
36. Fanning AS, Wolenski JS, Mooseker MS, Izant JG. Differential regulation of skeletal muscle myosin-II and brush border myosin-I enzymology and mechanochemistry by bacterially produced tropomyosin isoforms. Cell Motil Cytoskeleton. 1994; 29:29–45. [PubMed: 7820856]

37. Brawley CM, Rock RS. Unconventional myosin traffic in cells reveals a selective actin cytoskeleton. Proc Natl Acad Sci USA. 2009; 106:9685–9690. [PubMed: 19478066]

38. Sage D, Neumann FR, Hediger F, Gasser SM, Unser M. Automatic tracking of individual fluorescence particles: application to the study of chromosome dynamics. IEEE Trans Image Process. 2005; 14:1372–1383. [PubMed: 16190472]

39. Kerssemakers JW, Munteanu EL, Laan L, Noetzel TL, Janson ME, Dogterom M. Assembly dynamics of microtubules at molecular resolution. Nature. 2006; 442:709–712. [PubMed: 16799566]

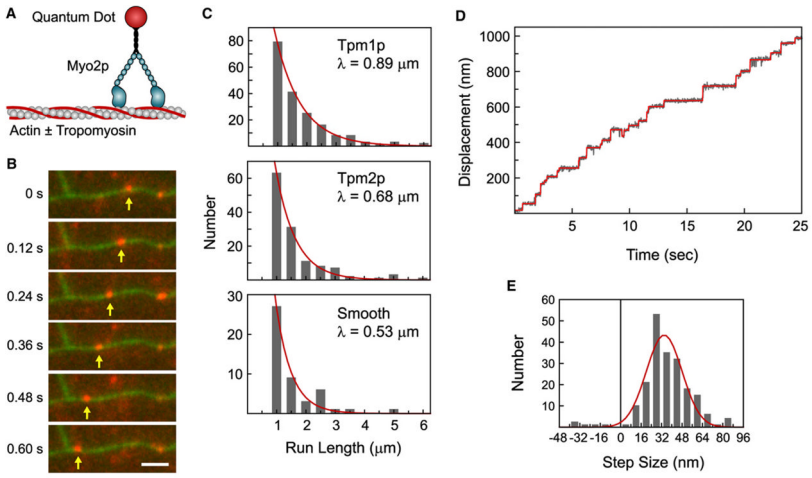

Figure 1.

Myo2p Moves Processively on Actin-Tropomyosin Filaments

(A) Schematic of the experimental setup.

(B) Time course of a Qdot-labeled Myo2p (red) moving processively on a Tpm1p-yeast actin filament (green). The time (in s) is shown to the left of each frame. The scale bar represents 2 μm. Yellow arrows indicate the moving Qdot.

(C) Histograms of run lengths for Myo2p with three different tropomyosin isoforms at 2mMMgATP. The x axis scale is identical for the three histograms. The red curve shows an exponential fit to determine the run length λ, which is shown for each isoform.

(D) Raw displacement versus time data of Myo2p stepping on actin-Tpm1p (gray) at 2 μMMgATP, with steps identified by a step-finding algorithm (red) [39].

(E) Histogram of step sizes. The step sizes are approximately Gaussian distributed, centered at 34.1 ± 1.3 nm (mean ± SE).

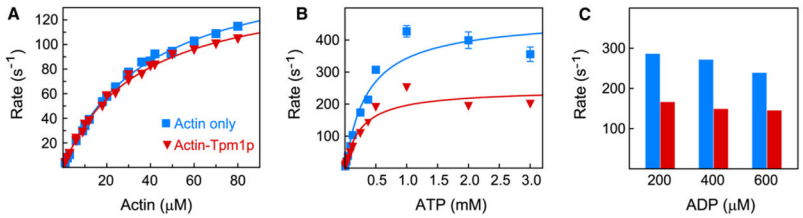

Figure 2.

Effects of Tpm1p on Myo2p-2IQ Kinetics

(A) Steady-state actin-activated ATPase activity as a function of actin concentration with skeletal muscle actin only (blue squares) or skeletal muscle actin plus Tpm1p (red triangles). Solid lines are fits to Michaelis-Menten kinetics. V_{max} = 171 ± 4 s^{-1} (actin), V_{max} = 151 ± 4 s^{-1} (actin -Tpm1p), K_M = 39 ± 2 μM (actin), K_M = 34 ± 2 μM (actin-Tpm1p). Fitted values are shown with SE. Data from two independent trials were combined.

(B) Tpm1p reduces the rate of ATP-induced dissociation of Myo2p from actin. Light scattering was used to follow the MgATP-induced dissociation of Myo2p-2IQ from skeletal muscle actin (blue squares) or skeletal muscle actin plus Tpm1p (red triangles) as a function of MgATP concentration. Solid lines show fits to a rectangular hyperbola to determine maximal ATP binding rate. Tpm1p causes a 47% reduction in the maximal rate of ATP binding and motor dissociation from actin (k_{max} = 467 ± 39 s^{-1}, actin only; k_{max} = 246 ± 22 s^{-1}, actin-Tpm1p). The initial slope defines a second order binding constant of~1 × 10^6 $M^{-1}sec^{-1}$, which was independent of the presence of tropomyosin. Data from one preparation are shown, but essentially identically values were obtained from an independent preparation of Myo2p-2IQ.

(C) Tpm1p reduces the apparent ADP dissociation rate. Acto.Myo2p-2IQ.ADP (±Tpm1p) was mixed with 6 mM MgATP, and light scattering was used to determine the apparent ADP dissociation rate at three initial ADP concentrations. The observed rate is lower for actin-Tpm1p (red) than actin only (blue). Because the rate of ATP-induced dissociation of the actin-Myo2p complex is low, the apparent ADP dissociation rate includes contributions from ATP binding as well. Rates from two independent trials were combined.

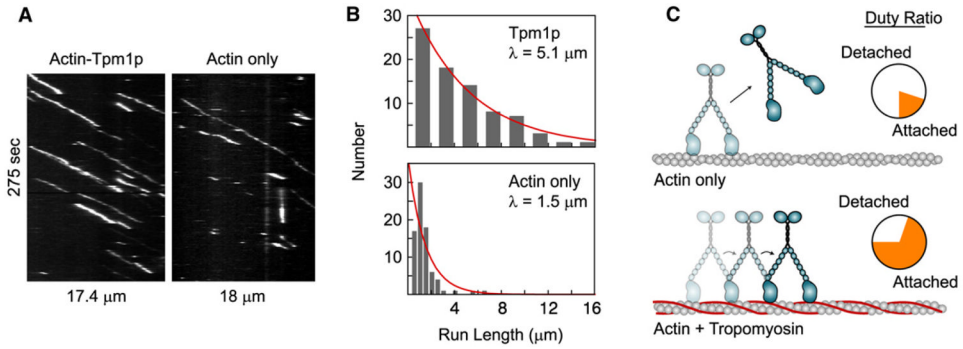

Figure 3.

At 10 μM ATP, Myo2p Is Able to Move Processively on Bare Actin, but Tpm1p Increases Run Lengths

(A) Kymographs showing Myo2p movement on Tpm1p-yeast actin versus bare yeast actin filaments. The slope of the white lines equals the speed, which is not affected by Tpm1p. The length of the lines represents run lengths, which are much longer with Tpm1p.

(B) Histograms of Myo2p run lengths with and without Tpm1p. The x axis scale is identical for both histograms. The red curve shows an exponential fit to determine the run length λ, which is shown for each isoform.

(C) Tropomyosin increases the duty ratio of Myo2p, the fraction of time each head spends strongly bound to actin. On bare actin at millimolar ATP concentration, Myo2p has a duty ratio of less than 50% and is not processive. On tropomyosin-actin filaments, the duty ratio is greater than 50% due to a slowing of the ADP release rate, and Myo2p becomes processive [23].

Table 1

Speed, Run Length, and Run Frequency of Myo2p with 2 mM MgATP

Actin	Tropomyosin	Speed[a] (μm/s)	Run Length[b] (μm)	Run Frequency[c]	N[d]
yeast	none	-	-	0	0
yeast	Tpm1p	5.4 ± 1.1	0.89 ± 0.04	39.6	255
yeast	Tpm2p	5.2 ± 1.2	0.68 ± 0.03	21.4	175
yeast	smooth muscle	4.6 ± 1.4	0.53 ± 0.07	3.0	96
skeletal muscle	none	-	-	0	0
skeletal muscle	Tpm1p	5.4 ± 1.3	0.77 ± 0.04	ND	110

[a] Mean ± SD.

[b] The characteristic run length, λ, was obtained by fitting $y = Ae^{-x/\lambda}$ to the run length histogram and is shown ± SE.

[c] Units are (μM Myo2p × μm actin × sec) $^{-1}$.

[d] Number of processive runs.